Published in final edited form as:
Circulation. 2003 December 9; 108(23): 2899–2904.

Magnetic Resonance Fluoroscopy Allows Targeted Delivery of Mesenchymal Stem Cells to Infarct Borders in Swine

Alexander J. Dick, MD, **Michael A. Guttman, MS***, **Venkatesh K. Raman, MD***, **Dana C. Peters, PhD**, **Breno S.S. Pessanha, MD**, **Jonathan M. Hill, MD**, **Scott Smith, PhD**, **Greig Scott, PhD**, **Elliot R. McVeigh, PhD**, and **Robert J. Lederman, MD**

From the Cardiovascular Branch (A.J.D., V.K.R., B.S.S.P., J.M.H., R.J.L.) and Laboratory of Cardiac Energetics, Division of Intramural Research (M.A.G., D.C.P., E.R.M.), National Heart, Lung, and Blood Institute, National Institutes of Health, Bethesda, Md, and Boston Scientific Corporation, Plymouth, Minn (S.S., G.S.).

Abstract

Background—The local environment of delivered mesenchymal stem cells (MSCs) may affect their ultimate phenotype. MR fluoroscopy has the potential to guide intramyocardial MSC injection to desirable targets, such as the border between infarcted and normal tissue. We tested the ability to (1) identify infarcts, (2) navigate injection catheters to preselected targets, (3) inject safely even into fresh infarcts, and (4) confirm injection success immediately.

Methods and Results—A 1.5-T MRI scanner was customized for interventional use, with rapid imaging, independent color highlighting of catheter channels, multiple-slice 3D rendering, catheter-only viewing mode, and infarct-enhanced imaging. MRI receiver coils were incorporated into guiding catheters and injection needles. These devices were tested for heating and used for targeted MSC delivery. In infarcted pigs, myocardium was targeted by MR fluoroscopy. Infarct-enhanced imaging included both saturation preparation MRI after intravenous gadolinium and wall motion. Porcine MSCs were MRI-labeled with iron-fluorescent particles. Catheter navigation and multiple cell injections were performed entirely with MR fluoroscopy at 8 frames/s with 1.7×3.3×8-mm voxels. Infarct-enhanced MR fluoroscopy permitted excellent delineation of infarct borders. All injections were safely and successfully delivered to their preselected targets, including infarct borders. Iron-fluorescent particle–labeled MSCs were readily visible on delivery in vivo and post mortem.

Conclusions—Precise targeted delivery of potentially regenerative cellular treatments to recent myocardial infarction borders is feasible with an MR catheter delivery system. MR fluoroscopy permits visualization of catheter navigation, myocardial function, infarct borders, and labeled cells after injection.

Keywords

magnetic resonance imaging; cells; drugs; myocardial infarction; catheterization

Successful myocardial regeneration by therapeutic mesenchymal stem cell (MSC) injection may be determined by the local tissue context of cell deposition. Wang et al[1] observed that

Correspondence to Robert J. Lederman, MD, Cardiovascular Branch, Clinical Research Program, Division of Intramural Research, National Heart, Lung, and Blood Institute, National Institutes of Health, Building 10, Room 2c713, Bethesda, MD 20892-1538. E-mail lederman@nih.gov.

*These authors contributed equally to this work.

Dr Smith is an employee of and Dr Scott is a consultant to Boston Scientific, Inc, which commercializes Stiletto endomyocardial injection catheters.

The online-only Data supplement is available at http://www/circulationaha.org

delivered diffusely, MSCs assume a fibroblast-like morphology within areas of myocardial infarction but a cardiomyocyte-like morphology within bordering normal myocardial tissue. The border between normal and infarcted tissue may represent a suitable environment for engraftment and cardiomyogenic differentiation.[2] It may be useful, therefore, to deliver MSCs directly to this border region.

We recently demonstrated that interactive MR fluoroscopy can guide injections in real time into a healthy beating heart.[3] Successful clinical MR fluoroscopy procedures, however, will require considerably more functionality. The procedure must be rapid and robust. Target tissue must be identifiable on the basis of anatomy, function, and/or tissue characteristics in real time. Injection success or failure should be evident immediately. Injections must be safe, avoiding perforation even early after myocardial infarction, and catheters must not heat inductively in the MRI environment.

In this feasibility study, we test the hypotheses that (1) infarct borders can be identified in real time; (2) catheters can be navigated to deliver injections to specified border, normal, or infarcted tissue rapidly and reliably; (3) injected MSCs can immediately be identified under MR fluoroscopy during and after injection; and (4) injections can be conducted safely even into freshly infarcted myocardium.

Methods

Animals

Animal protocols were approved by the National Heart, Lung, and Blood Institute Animal Care and Use Committee. Closed-chest myocardial infarctions were created in 10 Hanford miniswine (30 to 60 kg; Sinclair Research, Columbia, Mo). Animals received aspirin, atenolol, and lisinopril daily. Anesthesia was induced with ketamine and xylazine and maintained with isoflurane and mechanical ventilation. Heparin, amiodarone, and lidocaine were administered intravenously after percutaneous transfemoral access. Occlusive platinum coils (VortX, 2.5 to 3.5 mm; Boston Scientific) were delivered to the left anterior descending coronary artery after the second diagonal branch under x-ray guidance. This reproducibly caused a transmural infarction of the anterior wall, septum, and apex. To cause a small nontransmural infarction in 1 animal, an angioplasty balloon (Open-Sail 2.5×15 mm, Guidant) was inflated in the distal left anterior descending coronary artery for 60 minutes before reperfusion. In vivo thermometry was performed in an additional naive pig.

Cell Preparation and Labeling

Allogeneic porcine MSCs were isolated from bone marrow aspirates, expanded,[4] and then labeled with dual-contrast particles.[5] MSCs were incubated for 18 to 24 hours with 0.9-μm polystyrene beads containing 62% magnetite as an MRI marker and Dragon Green fluorescent dye as a histological marker (Iron-Fluorescent Particles, IFP, Bangs Laboratories). Injection mixtures included final concentrations of 1×10^6 to 2×10^6 labeled cells, tissue fast dye (Triangle Biomedical Sciences) diluted to 150 μL in PBS. Test injections used gadolinium-DTPA 30 mmol/L (Magnevist, Berlex).

Cell injections were conducted 1 to 7 days after myocardial infarction to simulate susceptibility to catheter rupture of nonreper-fused myocardial infarction. Three or 4 injections of labeled cells were performed in each of 10 animals. Needle dead space was cleared with saline before each needle retraction. Animals were killed and injection sites formalin-fixed or snap-frozen for histological examination.

Histopathology

We obtained serial representative 8-μm-thick sections of injection regions identified by tissue fast dye. Immunohistochemistry specimens were stained for desmin, with DAPI nuclear counterstain, and imaged under fluorescence, differential-phase, or light microscopy.

Custom MR Fluoroscopy Environment

A 1.5-T clinical MRI scanner (CV/i, General Electric) was customized with an external subsystem (Onyx2, Silicon Graphics) for real-time reconstruction of raw scanner data.[3,6] The scanner and external work station were controlled from a pair of in-room keyboards and shielded liquid crystal displays. Four independent high-impedance surface coils (Nova Medical) were used interchangeably with intravascular coils (see below). The suite was equipped with an MR-compatible patient-monitoring system providing display of oximetry, instantaneous blood pressure, and ECG.

An external subsystem extended the commercial real-time graphical user interface (i-Drive, General Electric) with interactive scan and reconstruction control features significantly enhanced from a previous iteration.[3] Gain and color highlighting of signals from each receiver channel can be adjusted independently. Image acceleration techniques and temporal resolution controls can be adjusted interactively (see Acquisition Parameters). Magnetization preparation pulses can be activated, including nonselective water or fat saturation. ECG gating can be toggled on/off. A catheter-channel-only projection imaging mode was developed to show catheter position even when outside the thin-slice imaging plane.[7] To visualize the complex interrelation of anatomy, function, catheter position, and intramyocardial injectate distribution, a multislice acquisition mode was implemented having 3D-rendered reconstructions of translucent slices.[8]

MR Fluoroscopy Acquisition Parameters

All injections were guided by steady-state free precession sequences (RT-SSFP),[9] run in fluoroscopic (real-time) mode, with either rectilinear or radial k-space trajectories. For rectilinear trajectories, image-acceleration techniques were applied, such as echo sharing, in which acquisitions were alternated between even and odd phase-encoding lines with temporal filtering similar to that in UNFOLD,[10] generating 8 frames/s and an acquisition-to-display latency of ≈250 ms. Typical rectilinear imaging parameters were repetition time (TR), 3.8 ms; time to echo (TE), 1.9 ms; flip angle, 60°; bandwidth, ±62.5 kHz; 192×96 matrix; 32×24-cm field of view; ¾ partial-phase acquisition generating 1.7×2.5×8-mm voxels. For radial trajectories, image acceleration was achieved by use of undersampling of projection views.[7] The user interactively adjusted the compromise between temporal resolution and image quality by varying the amount of undersampling.[7] Typical radial imaging parameters were TR, 4.0 ms; TE, 1.9 ms; flip angle, 60°; bandwidth, ±62.5 kHz; 160×64 projections; 32-cm field of view; generating 2×2×8-mm voxels. MSC injection sites were also inspected by use of segmented, ECG-gated, breath-held fast gradient echo: TR, 6.5 ms; TE, 2.9; flip angle, 15°; bandwidth, ±31.5 kHz; 256×128 matrix; 34×34-cm field of view; ¾ phase acquisition generating 1.3×2.7×8-mm voxels; and SSFP MRI: TR, 4.8 ms; TE, 1.9; flip angle, 60°; bandwidth, ±62.5 kHz; 256×128 matrix; 34×34-cm field of view; ¾ phase acquisition generating 1.3×2.7×8 mm voxels.

MR Fluoroscopy of Myocardial Infarction

Infarcted targets were identified by impaired myocardial thickening during RT-SSFP MR fluoroscopy and by contrast enhancement. Although infarcted tissue is visible in RT-SSFP imaging without contrast agent, blood-to-infarct contrast is poor. To improve this contrast, delayed hyperenhancement (DHE) was used in conjunction with a 90° nonselective saturation

pulse played before each echo-shared image (sat-RT-SSFP). DHE of the infarcted region was created by injecting Gd-DTPA 0.2 mmol/kg via a peripheral intravenous line 20 to 60 minutes before imaging. This non–ECG-gated, free-breathing technique was compared with RT-SSFP and with conventional segmented, ECG-gated, breath-held inversion recovery gradient echo (IR-GRE) DHE as the reference standard for identification of infarcted tissue.[11]

Injection Catheters and Their Use

The coaxial ("guide-in-guide") 9F transfemoral guiding catheter system and injection needle (MRI-modified Stiletto 2, Boston Scientific Corporation) were adapted to serve as MRI receiver coils in parallel with surface coils. The MRI receiving coil and transmission line were integrated into the guiding catheter. An additional receiver coil was added immediately proximal to the Stiletto needle tip to generate a high-intensity signal on a separate receiver channel.

Guiding catheters were advanced across the aortic valve over nitinol guidewires. Three injection regions were predetermined and targeted in each animal: infarcted nonviable myocardium, border between infarcted and normal myocardium, and normal myocardium. ECG, instantaneous pressure, and real-time images of cardiac motion were monitored continuously.

Safety Testing

Intravascular MRI receiver coils can potentially heat during scanning.[12] Catheter heating was tested[13] with a 4-channel fluoroptic thermometer (model 3100, Luxtron). Probes were attached at the tips of the 9F left ventricular (LV) sheath, coaxial LV steering guide, and Stiletto, respectively. A reference probe measured the bath (in vitro) or core body (in vivo) temperature. Static phantoms, intended to exaggerate heating, included a 8×110-cm tube (small heat sink) and a 10-L tub (large heat sink), each filled with normal saline, with the catheter positioned in the isocenter or closer to the RF transmitter (20 cm off center of the 60-cm diameter bore, to increase susceptibility to heating). Recordings were also obtained in the iliac artery, aortic root, and LV cavity of a naive pig. Temperature fluctuations were recorded during continuous SSFP TR, 3.8 ms;α, 60° to 90°; with and without saturation preparation, for 120 seconds after steady state was achieved, typically 150 to 300 seconds. Worst-case scenarios for heating were also simulated by disconnecting one or both of the catheter coils from the MRI receivers.

Data Analysis

Infarct hyperenhancement methods (RT-SSFP, sat-RT-SSFP, and IR-GRE) were compared by use of contrast-to-noise ratios between normal myocardium, infarcted myocardium, and blood by 2 independent observers. Regions of interest were placed within the normally contracting septum ≈10 mm from the infarct border (normal), within the akinetic apical infarct wall ≈10 mm from the infarct border, and within the LV cavity (blood). Real-time wall thickening and the location, depth (center of mass), and intramyocardial distribution of susceptibility artifacts corresponding to stem-cell injections were analyzed offline (Medical Imaging Processing, Analysis and Visualization, v0.99, NIH). Continuous parameters are expressed as mean±SD.

Results

Infarct Identification

Myocardial infarctions and their borders were clearly identifiable under MR fluoroscopy by patterns of myocardial contraction. Using image acceleration, 8 frames/s allowed satisfactory wall-motion assessment over several cardiac cycles. Akinetic and normal segments were easily differentiated in all 10 animals. Stored MR fluoroscopy images were analyzed post hoc in 6

animals and revealed average regional thickening of −2±3% in the infarct, 47±8% in normal lateral walls, and 36±4% in normal septum.

Myocardial infarctions were also clearly identifiable on the basis of contrast characteristics. Before intravenous injection of Gd-DTPA, infarcted myocardium was slightly brighter than normal myocardium in RT-SSFP images. Approximately 15 minutes after the injection, DHE increased the contrast between normal and infarcted myocardium to allow targeting for up to 120 minutes. Figure 1 compares MR fluoroscopic (sat-RTSSFP and RT-SSFP) with conventional (IR-GRE) DHE images of the same slice. Infarcted and normal myocardium could be differentiated by all techniques, but the ability to differentiate blood in the LV cavity from infarcted myocardium was poor with RT-SSFP (Table) without the application of a saturation pulse. Dysfunctional segments corresponded exactly to regions of DHE in this animal model.

Catheter Operation and Targeting

Guiding catheters were introduced into the LV under RT-SSFP guidance using color highlighting (green) of signal from the built-in coil. Preselected normal, infarct, or border targets were identified by regional wall motion and DHE. Catheter manipulations were visualized with RT-SSFP and were facilitated by toggling catheter-only mode (Figure 2) when part of the catheter moved out of the selected imaging slice and by 3D rendering of multislice acquisitions to portray complex anatomic relationships. Next, the Stiletto was inserted and extended beyond the tip of the guiding catheter to engage the targeted myocardium. Needle purchase was confirmed by 50- to 150-μL test injections of 30 mmol/L Gd-DTPA, after toggling saturation preparation, looking for localized hyperenhancement, which was brighter than the surrounding normal or hyperenhanced myocardial infarction. A representative injection sequence is shown in Figure 3. For portions of the active guiding catheter in the imaging plane, the lumen was visible as a dark stripe with color-highlighted regions (green) on either side. Portions of the catheter that were near but not in the imaging plane were still visible as color-highlighted regions. Thus, the sensitivity profile of the active guiding catheter was used interactively to optimize the imaging plane position and orientation. Satisfactory myocardial purchase was demonstrated reproducibly by apposition of the deployed needle coil with myocardium and by mechanical feedback to the operator. To test the precision of infarct border targeting, a very small infarct (12×8×8 mm) was created. Multislice MR fluoroscopy permitted cells to be positioned precisely along the apical and basal borders of this infarct (Figure 4 and online-only Data Supplement).

Visualization of Cell Injections

A total of 34 MSC injections were conducted with MR fluoroscopy guidance into prespecified normal, infarcted, or border targets. The 2-channel catheter and Stiletto delivery system permitted successful visualization of injections in 100% of attempts, compared with 81% with an earlier generation system in which only the catheter contained a receiver coil.[3] By MRI and by gross pathology, 15 of 15 injections intended for infarct were delivered into the infarcted nonviable myocardium, 12 of 12 intended for the border of normal and infarct, and 7 of 7 intended for normal myocardium remote to the infarct.

MSC injections were all immediately apparent under MR fluoroscopy as localized reduction in signal (dark pixels) attributed to intracellular iron label (Figure 5). Orthogonal (long- and short-axis) views were acquired in real time to observe intramyocardial deposition of the labeled MSCs. Injections containing as few as 1×10^6 IFP-labeled MSCs were readily visualized. The intramyocardial distributions of these injections varied depending on the location of delivery. Susceptibility artifacts corresponding to injections had the following

subendocardial depths: 2.6±0.6 mm within infarct, 3.0±0.6 mm at the infarct border, and 4.3 ±4.5 mm in normal myocardium remote to the infarct.

Injection sites were localized on gross pathology by tissue fast stains on the endocardial surface. Histological examination was performed on 17 of 34 injections. Intact IFP-labeled stem cells were evident at injection sites on postmortem microscopy (Figure 5, B and E). Desmin staining of intact myocardium highlighted the border location of delivered cells.

Safety

In the tub phantom and in vivo in all positions, negligible heating (0.2°C) was observed during continuous RT-SSFP scanning, even when the catheter coils were deliberately disconnected from the scanner or placed close to the bore wall. However, when the catheter coils were tested in a small heat-sink phantom (narrow tube of uncirculated saline), temperature rose as much as 3.2°C. Background temperature measurements fluctuated by 0.2°C (SD).

Endomyocardial contact of either the catheter or the Stiletto occasionally caused transient ventricular premature contractions. At a heart rate of 70±20 bpm, 8 frames/s permitted ready ectopy detection, facilitating immediate catheter repositioning when necessary. No other ectopy was observed after interstitial deposition of 150 μL cellular injection mixtures in normal, infarcted, or border tissue. In one animal, exit of the 27-gauge needle (but not the catheter) was visualized as a rapidly clearing hyperintensity during the first test injection of gadolinium into the apical infarct region. The needle was withdrawn, and this animal underwent 3 injections at other sites. There was no pericardial effusion during 6 hours of subsequent imaging or on immediate postmortem examination.

Discussion

These experiments demonstrate a complex procedure allowed by the use of many newly developed MR fluoroscopy techniques. Infarct borders were precisely delineated, catheters navigated in 3D space, and labeled cellular agents safely and effectively delivered into the prespecified midmyocardial segments under direct observation.

Intramyocardial Delivery

Transcatheter intramyocardial injection will most likely be useful for clinical delivery of MSCs and other emerging cellular therapies. Depositing cells into the myocardial inter-stitium may circumvent the requirement that intravenously or intra-arterially administered cells home to target tissue on the basis of poorly understood signaling processes. Precise targeting of myocardial injections based on tissue viability, eg, the border between healthy and infarcted myocardium, could be important for efficacy. Even after direct injection, a large fraction of injected material may immediately exit the myocardium.[14,15] Although iron labeling most likely exaggerates the volume of delivered cells, we demonstrate that magnetic labeling of stem cells permits immediate confirmation of successful delivery and precise localization in vivo. However, the size of signal voids in vivo is probably not proportional to cell quantity; therefore, this technique is limited in ability to visualize early injectate loss. IFP and other labeling techniques[16] may prove useful to trace the distribution of injected cells in the beating heart.

Real-Time Functional Assessment of Myocardium

Online regional functional myocardial assessment was performed in these pig experiments with real-time SSFP, and the findings were satisfactory to target therapy delivery. This was possible without breath holding or ECG gating. The imaging rate of 8 frames/s was adequate to provide a useful qualitative assessment of myocardial contractility. In addition, saturation preparation after systemic Gd-DTPA administration provided additional contrast between

infarcted myocardium and blood that was crucial for targeting delivery. Further study will be necessary to determine the usefulness of this technique in determining infarct size.

Active Catheters

The "active" catheters we used, so designated because they serve as radiofrequency MRI antennas and receive signal from nearby blood and tissue, proved essential in these experiments. For example, color highlighting of the catheter and needle tip signals markedly improved operator confidence in needle position and purchase. Interactive catheter-only display was helpful to visualize the catheter when outside the selected imaging slice. "Passive" catheters, such as ferromagnetic coronary stents[17] and atrial septal occluder devices,[18,19] are visualized as signal voids (black spots) and are not amenable to such interventional imaging enhancements.

Safety

Conductive catheters are capable of heating, especially during MRI radiofrequency excitation. Several approaches have been reported for shielding or decoupling active catheters to prevent heating.[20,21] We found that our MRI catheters did not heat appreciably during prolonged radiofrequency exposure in vivo. Worst-case heating simulations using a low-heat-sink phantom tube caused heating up to 3.2°C. These remain within FDA guidelines (specific absorption rate, 8 W/g; whole-body temperature increase, <1°C).[22]

This seems to be the first report of transcatheter injections into freshly infarcted myocardium. Intramyocardial deposition of small 150-μL volumes did not cause sustained tachycardia. One needle (but not catheter) extended through a thin apical wall without sequelae; no significant perforations were observed.

Alternative Technologies

Several alternative technologies allow endomyocardial injections. Transesophageal and intracardiac ultrasound systems have been used to guide direct transcatheter myocardial gene transfer.[23] Ultrasound imaging is limited by "black-out" regions created by device shadows. Electromechanical navigation and injection systems, which overlay a position sensor onto a previously acquired endocardial roadmap, can guide myocardial drug delivery.[24] However, the spatial precision of this approach is controversial, given the coarse "road mapping" over previously acquired moving images. Moreover, injection success and intramyocardial distribution cannot be assessed with electromechanical mapping.

Conclusions

We describe new interactive interventional features, such as real-time infarct-enhanced imaging, 3D-rendered multislice display, and catheter-only projection mode, that permit robust catheter navigation and precise and safe injection targeting around fresh infarcts with immediate feedback of success. Although this functionality is not yet commercially available, the technologies used are widely obtainable. By providing continuous information on interventional device position, local myocardial function, and myocardial viability, MR fluoroscopy allows targeted intramyocardial delivery and tracking of potential regenerative stem cell therapies.

Supplementary Material

Refer to Web version on PubMed Central for supplementary material.

Acknowledgements

We are grateful to Kevin Edmunds and Ken Larson of Boston Scientific for catheter development; Peter Kellman for designing the surface coils; Zu-Xi Yu for histological preparations and microscopy; Dan Ennis for volume renderings; Joni Taylor, Diana Lancaster, and Gina Orcino for veterinary assistance; Annette Stine for logistical support; and Toren Finkel and Robert Balaban for helpful comments and suggestions.

References

1. Wang JS, Shum-Tim D, Chedrawy E, et al. The coronary delivery of marrow stromal cells for myocardial regeneration: pathophysiologic and therapeutic implications. J Thorac Cardiovasc Surg 2001;122:699–705. [PubMed: 11581601]
2. Orlic D, Kajstura J, Chimenti S, et al. Bone marrow cells regenerate infarcted myocardium. Nature 2001;410:701–705. [PubMed: 11287958]
3. Lederman RJ, Guttman MA, Peters DC, et al. Catheter-based endomyocardial injection with real-time magnetic resonance imaging. Circulation 2002;105:1282–1284. [PubMed: 11901036]
4. Pittenger MF, Mackay AM, Beck SC, et al. Multilineage potential of adult human mesenchymal stem cells. Science 1999;284:143–147. [PubMed: 10102814]
5. Hill J, Dick A, Raman V, et al. Serial cardiac magnetic resonance imaging (MRI) of injected mesenchymal stem cells. Circulation 2003;108:1009–1014. [PubMed: 12912822]
6. Guttman MA, McVeigh ER. Techniques for fast stereoscopic MRI. Magn Reson Med 2001;46:317–323. [PubMed: 11477636]
7. Peters D, Lederman R, Dick A, et al. Interactive undersampled projection reconstruction for active catheter imaging, with adaptable temporal resolution and catheter-only views. Magn Reson Med 2003;49:216–222. [PubMed: 12541240]
8. Guttman MA, Lederman RJ, Sorger JM, et al. Real-time volume rendered MRI for interventional guidance. J Cardiovasc Magn Reson 2002;4:431–442. [PubMed: 12549231]
9. Oppelt A. FISP: a new fast MRI sequence. Electromedica 1986;54:15–18.
10. Madore B, Glover GH, Pelc NJ. Unaliasing by Fourier-encoding the overlaps using the temporal dimension (UNFOLD), applied to cardiac imaging and fMRI. Magn Reson Med 1999;42:813– 828. [PubMed: 10542340]
11. Kim RJ, Fieno DS, Parrish TB, et al. Relationship of MRI delayed contrast enhancement to irreversible injury, infarct age, and contractile function. Circulation 1999;100:1992–2002. [PubMed: 10556226]
12. Yeung CJ, Susil RC, Atalar E. RF safety of wires in interventional MRI: using a safety index. Magn Reson Med 2002;47:187–193. [PubMed: 11754458]
13. Nitz WR, Oppelt A, Renz W, et al. On the heating of linear conductive structures as guide wires and catheters in interventional MRI. J Magn Reson Imaging 2001;13:105–114. [PubMed: 11169811]
14. Grossman PM, Han Z, Palasis M, et al. Incomplete retention after direct myocardial injection. Cathet Cardiovasc Interv 2002;55:392–397.
15. Rezaee M, Yeung AC, Altman P, et al. Evaluation of the percutaneous intramyocardial injection for local myocardial treatment. Cathet Cardiovasc Interv 2001;53:271–276.
16. Bulte JW, Douglas T, Witwer B, et al. Magnetodendrimers allow endosomal magnetic labeling and in vivo tracking of stem cells. Nat Biotechnol 2001;19:1141–1147. [PubMed: 11731783]
17. Spuentrup E, Ruebben A, Schaeffter T, et al. Magnetic resonance– guided coronary artery stent placement in a swine model. Circulation 2002;105:874– 879. [PubMed: 11854130]
18. Buecker A, Spuentrup E, Grabitz R, et al. Magnetic resonance-guided placement of atrial septal closure device in animal model of patent foramen ovale. Circulation 2002;106:511–515. [PubMed: 12135954]
19. Rickers C, Jerosch-Herold M, Hu X, et al. Magnetic resonance image-guided transcatheter closure of atrial septal defects. Circulation 2003;107:132–138. [PubMed: 12515755]
20. Ladd ME, Quick HH. Reduction of resonant RF heating in intravascular catheters using coaxial chokes. Magn Reson Med 2000;43:615– 619. [PubMed: 10748440]
21. Yeung CJ, Atalar E. RF transmit power limit for the barewire loopless catheter antenna. J Magn Reson Imaging 2000;12:86–91. [PubMed: 10931568]

22. *Guidance for Industry: Guidance for the Submission of Premarket Notifications for Magnetic Resonance Diagnostic Devices*. Rockville, Md: Center for Devices and Radiological Health, US Food and Drug Administration; 1998.

23. Park SW, Gwon HC, Jeong JO, et al. Intracardiac echocardiographic guidance and monitoring during percutaneous endomyocardial gene injection in porcine heart. Hum Gene Ther 2001;12:893–903. [PubMed: 11387055]

24. Oron U, Halevy O, Yaakobi T, et al. Technical delivery of myogenic cells through an endocardial injection catheter for myocardial cell implantation. Int J Cardiovasc Intervent 2000;3:227–230. [PubMed: 12431347]

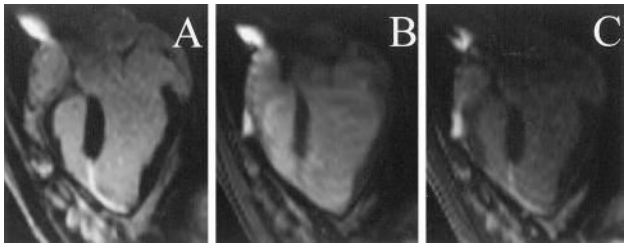

Figure 1.
Comparison of Gd-DTPA–enhanced infarct-imaging techniques. A, Conventional IR-GRE DHE. B, Real-time steady-state free precession. Infarcted tissue is visible but difficult to distinguish from LV cavity blood. C, Real-time steady-state free precession with a saturation prepulse (sat-RT-SSFP). DHE is visible by real-time methods without ECG gating or breath holding. Saturation prepulse improves real-time delineation of endo-cardial infarct border.

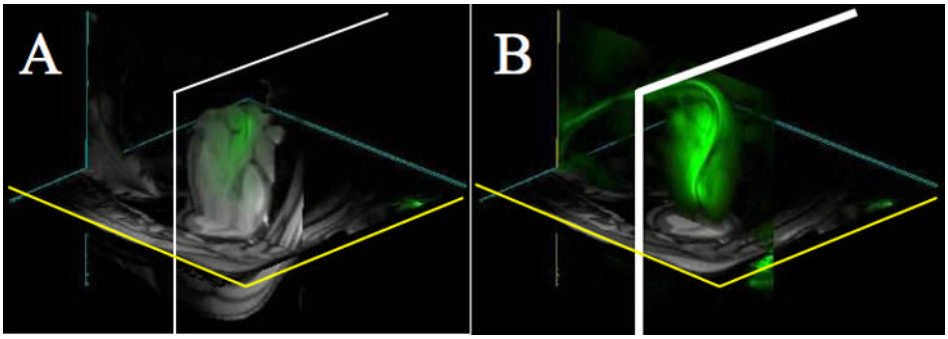

Figure 2.
Catheter tracking using 3D multislice MR fluoroscopy: A, Thin slice of catheter (green) within LV. Distal end is outside of scan plane and therefore not visible. B, By switching to a catheter-only mode, entire catheter becomes visible, analogous to x-ray projection.

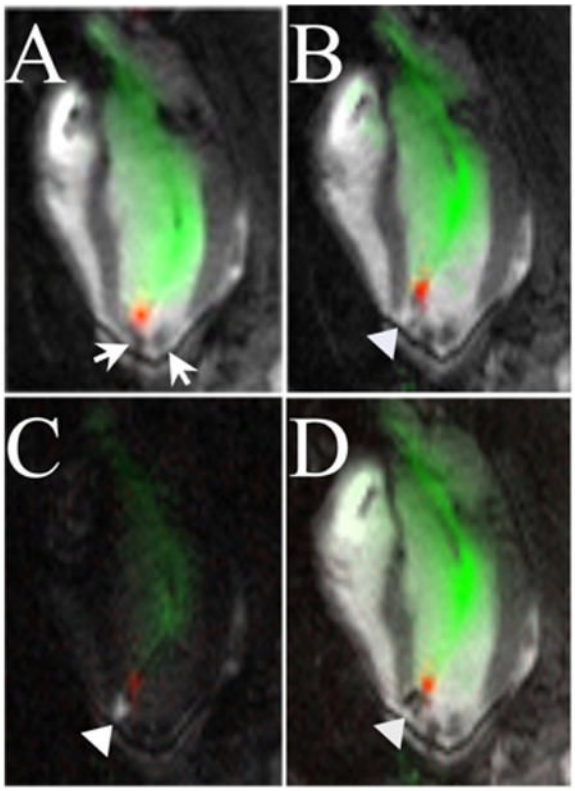

Figure 3.

MR fluoroscopy injection sequence. A, Stiletto is engaged at apical septal border of anterior myocardial infarction. MRI signal from needle tip is red and that from guiding catheter green. Arrows indicate previous injections of iron-labeled stem cells, which show as dark signal voids. B, A 150-μL test injection of Gd-DTPA is indicated by arrowhead and shows as white. C, Saturation-preparation enhances appearance of test injectate compared with black myocardium and blood. D, Iron-labeled MSCs (1×10^6) are injected into same spot, extinguishing local signal, and appear dark.

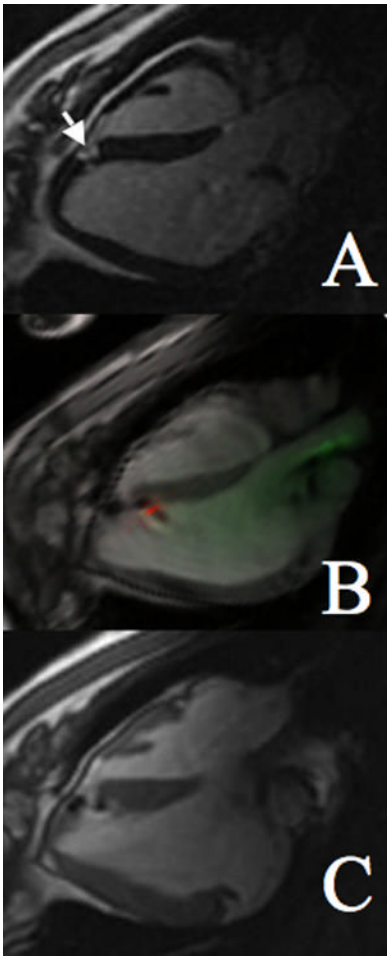

Figure 4.
Precise targeting of infarct border of a small infarct. A, Conventional inversion recovery DHE showing small area of infarction (arrow). B, Real-time steady-state free precession image of second injection into infarct border. C, Postinjection high-resolution gated, breath-held steady-state free precession image clearly showing 2 border injections.

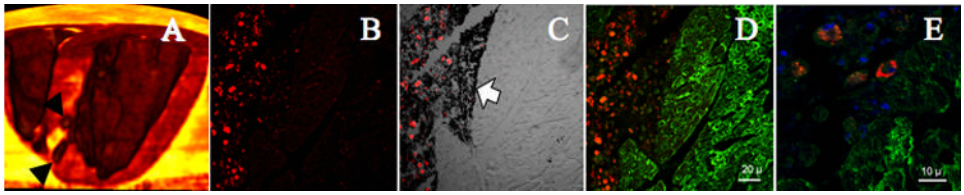

Figure 5.

A, 3D postmortem MRI shows injections (arrowheads) along border of infarct (bright yellow). B, Fluorescent micrograph of an infarct border shows red IFPs within injected MSCs. C, Differential phase image of same section shows tissue fast dye in black (arrow). Overlaying fluorescent image identifies IFP-labeled MSCs. D, Desmin stain of same section shows intact myocardium in green. E, Neighboring section shows perinuclear IFPs surrounding blue DAPI-stained nuclei within MSCs.

Table 1

Comparison of Infarct Imaging Techniques

Contrast-to-Noise Ratio	Real-Time Saturation Prepulse Steady-State Free Precession (sat-RT-SSFP) (n=6)	Real-Time Steady-State Free Precession (RT-SSFP) (n=6)	Conventional Inversion Recovery Hyperenhancement (IR-GRE-DHE) (n=6)
Infarct to normal myocardium	27±17	24±4	51±6
Infarct to blood	12±6	−5±5	19±13
Blood to normal myocardium	16±11	29±4	31±7

Contrast-to-noise ratio comparisons for 3 methods of DHE. Infarcted myocardium is visible in RT-SSFP after systemic Gd-DTPA injection. Saturation preparation decreases blood-to-myocardium contrast-to-noise ratio but improves blood-to-infarct contrast-to-noise ratio and thereby enhances the endocardial border delineation.